A Silicon Photonic Broken Racetrack Resonator for large-scale Tuning of FSR

Mehrdad Mirshafiei, Robert Brunner, Stephane Lessard, and David V. Plant, *Fellow, IEEE*

***Abstract*—We propose and demonstrate experimentally a novel racetrack resonator, in which the perimeter is broken into two sections that are coupled together by forming directional couplers. Simulation and experimental results confirm the performance of the broken racetrack geometry. We demonstrate that the free spectral range (FSR) of the resonator shrinks from 5.7 nm to 0.3 nm by testing 7 devices with discrete variations in displacement of the inner segment.**

***Index Terms*—Silicon photonics, racetrack resonator, optical filter, multiwavelength filter.**

I. Introduction

OPTICAL filters are essential components used in several applications including optical networks, microwave photonics, nonlinear optics, and optical sensing. Multiwavelength filters, which can process several optical channels simultaneously, can be built using various approaches including Fabry-Perot interferometers and microring resonators [1], [2]. Optical switches and electro-optical modulators based on microring resonators have also been demonstrated [3]. Because of their fixed dimensions, these filters have a constant free spectral range (FSR), where the FSR is defined as the wavelength spacing between two successive resonances in an interferometer.

A tunable FSR is beneficial in many applications, such as multiwavelength lasers and nonlinear optics. In [4], a microring was used to generate a frequency comb by four-wave mixing in a parametric process. Three different rings were fabricated to achieve comb sources with FSRs of 80, 40, and 20 GHz. A ring resonator with tunable FSR can replace these three devices to produce a tunable frequency comb.

Filters with a tunable FSR provide flexibility in an optical network. Future optical networks will use a flexible grid in which the channel spacing will change depending on the network conditions. In data center applications additional wavelengths will be used to increase data transmission capacity. More wavelengths means filters and switches with smaller FSRs are needed.

Tunability of FSR has been shown in a sampled chirped fiber Bragg grating filter [5], and on a silicon-on-insulator (SOI) platform by tuning the mutual coupling of two strongly coupled resonators using micro-heaters [6]. The former method is fiber-based and not an integrated solution, whereas the latter allows for limited FSR tunability.

M. Mirshafiei and D. Plant are with the Department of Electrical and Computer Engineering, McGill University, Montreal QC H3A 0E9, Canada e-mail: (mehrdad.mirshafiei@mcgill.ca).

R. Brunner and S. Lessard are with Ericsson Canada, Montreal QC H4P 2N2, Canada.

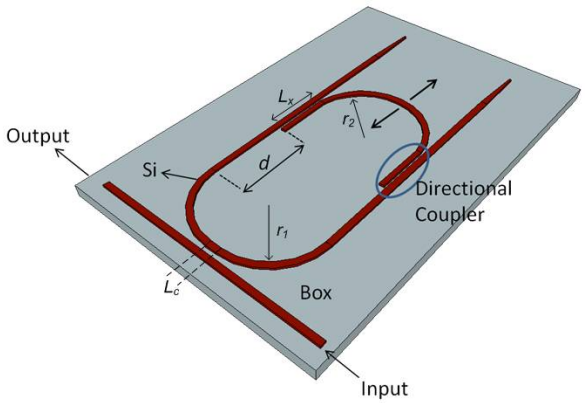

Fig. 1. Schematic diagram of the broken racetrack structure. d is the inner section displacement.

A microelectromechanical system (MEMS) based broken microring was demonstrated in [7], [8]. Using comb actuators to change the circumference of the microring by about a micrometer, resonant wavelength was shifted by 27 nm with no change in FSR. This approach is an alternative to thermo-optic shifting of microring resonance with better power efficiency.

In this letter, we propose a novel method to tune the FSR of a racetrack resonator on SOI platform by dividing the ring into two sections which are optically coupled but physically separate. Experimental results show that this configuration results in filters with good extinction ratios. We confirm the tunability of the FSR by fabricating several samples in which the inner section of the ring is discretely shifted. A MEMS based implementation could precisely move the inner arm and allow real-time control. An in-plane inchworm MEMS [9] is a suitable candidate to achieve the range of motion needed for large tuning of FSR.

II. Principle of Operation and Design of the Broken Racetrack Resonator

Fig. 1 presents a schematic view of the broken racetrack structure. The movable inner part of the ring is in close proximity to the fixed outer part to form directional couplers. The directional coupler is designed to be at the crossover length, L_x, to fully transfer light from one waveguide to the other. Since the directional coupler operates at a 100% coupling efficiency, light is contained inside the cavity at resonance and the total loss inside the ring is comparable to a typical microring. The two ends of the outer ring are tapered

TABLE I
DESIGN PARAMETERS

gap	100 nm	λ	1550 nm
r_1	11.5 μm	r_2	10.9 μm
L_c	3 μm	L_x	14.8 μm
n_1	2.4796	n_2	2.4270
Δn	0.0524	n_g	4.2
t	0.9		

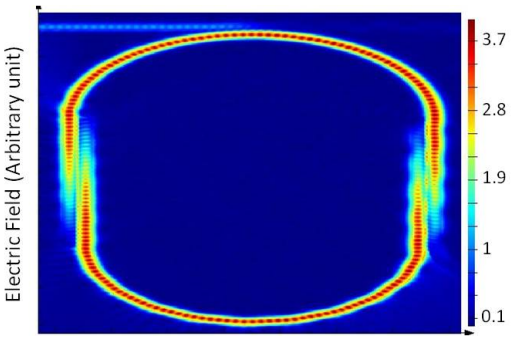

Fig. 2. FDTD simulation of the electric field in the broken racetrack at resonance.

down to 60 nm to attenuate any residual light and suppress back reflections.

The silicon strip waveguides are 500 nm wide and 220 nm high, sitting on a 2 μm thick SiO_2 box. A 2 μm SiO_2 cladding covers the waveguides. The gap between the input bus waveguide and the ring, and the directional coupler gap is 100 nm. We use a finite difference method to find the effective indices of the two supermodes in the directional coupler and the coupling coefficient. The crossover length of a coupler is $L_x = \lambda/(2\Delta n)$, where $\Delta n = n_2 - n_1$ is the difference between the effective indices of the two supermodes, and λ is the wavelength of light. The group index is found by $n_g = n_{eff} - \lambda dn_{eff}/d\lambda$, where n_{eff} is the effective index [10].

The directional coupler is analyzed in Lumerical MODE and FDTD. Table I shows the physical dimensions and the simulated design parameters, where r_1 and r_2 are the radius of the outer and the inner segments of the racetrack, L_c is the coupling region length and t is the coupler transmission coefficient. Fig. 2 shows the finite-difference time-domain (FDTD) simulation results for the electric field in the broken racetrack at resonance. The electric field couples from the outer arm to the inner arm with very little residual light escaping the cavity. A contour plot of the FSR versus the arm displacement and the radius is depicted in Fig. 3. Note that about 250 μm travel range is required to tune the FSR from 3.2 nm to 0.8 nm (400 GHz to 100 GHz).

III. EXPERIMENTAL RESULTS AND DISCUSSION

The device with the described parameters was fabricated using e-beam lithography. A tunable laser was coupled to the chip by vertical coupling using grating couplers. A back-to-back pair of grating couplers show 16 dB of insertion loss. The measured transmission frequency response of the racetrack

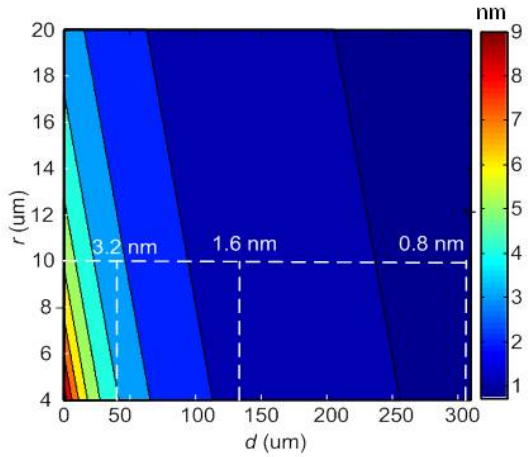

Fig. 3. FSR versus the racetrack radius and arm displacement.

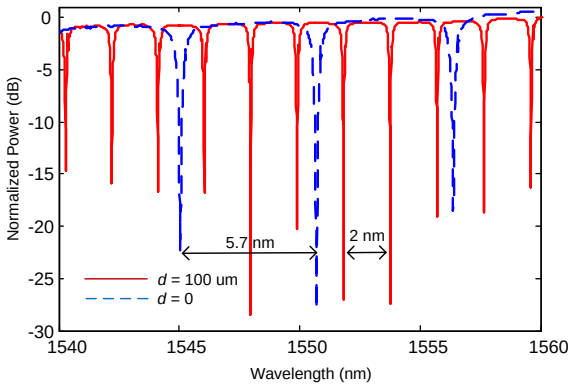

Fig. 4. Measured transmission response of the broken racetrack resonator for two displacement values of 0 and 100 μm.

resonator is plotted in Fig. 4 for two displacement values of 0 and 100 μm, shrinking the FSR from 5.7 nm to 2 nm. The transmission response is normalized to a back-to-back grating coupler response to remove the grating coupler contribution in the spectral response. We observe deep resonances around 1550 nm and weaker ones at other wavelengths.

The optical transmission intensity for an all-pass ring is

$$T = \frac{a^2 - 2atcos\phi + t^2}{1 - 2atcos\phi + (at)^2}, \tag{1}$$

where a is the round trip field loss coefficient in the cavity and ϕ is the single-pass phase shift [2]. The extinction ratio, ER, of a ring can be expressed as

$$ER = \frac{(t+a)^2}{(1+ta)^2} . \frac{(1-ta)^2}{(t-a)^2}. \tag{2}$$

The critical coupling in a microring occurs when the coupled power is equal to the power lost or $t = a$. Fig. 5 shows the extinction ratio of the broken racetrack resonator, calculated from (2), for displacement values of 0 and 50 μm. The measured transmission response and transmission response obtained from (1) are also plotted in Fig. 5. The limited bandwidth of the directional couplers used to couple the two segments of the resonator limits the wavelength span in

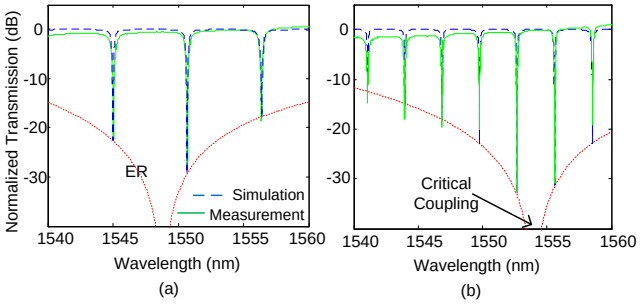

Fig. 5. Transmission response of the broken racetrack resonator for the displacement value of (a) 0 and (b) 50 μm. The measured transmission response is in green and the response obtained from (2) is shown in dashed blue line. Extinction ratio is plotted in dotted red.

which the resonator operates close to the critical coupling condition. We also notice a redshift in the wavelength for which critical coupling occurs in larger resonators. Larger resonators have more loss and require a smaller transmission coefficient to satisfy the critical coupling condition. The transmission coefficient decreases with an increase of wavelength resulting in a redshift in the critical coupling.

In a tunable multiwavelength filter, simultaneous control of the FSR and resonance wavelengths may be desired. A change in refractive index of silicon, induced by a thermo-optic effect, could provide tuning of resonance wavelengths in the racetrack resonator. Resonance wavelength can also be adjusted by a fine movement of the MEMS actuators as shown in [8]. A sub-micrometer change in the position of the MEMS part is enough to induce enough tuning of the resonance wavelength without any significant impact on the FSR.

The arm displacement is varied from 0 to 1000 μm in 7 discrete steps to study the tunability of the filter. Fig. 6 shows the FSR versus displacement. The solid blue line is the FSR obtained from the measurement of the 7 samples. The FSR can be expressed as

$$FSR = \frac{\lambda^2}{n_g.L}, \tag{3}$$

where L is the perimeter of the resonator [2]. The dashed red line in Fig. 6 is the FSR obtained from (3) with $n_g = 4.2$, which closely matches the experimental results. The FSR is tuned from 5.7 nm to 0.3 nm with a displacement of 1 mm.

The Quality factor, Q, of the resonator is defined as $Q = \lambda_{res}/\text{FWHM}$, where λ_{res} is the resonance wavelength and FWHM is the full width at half maximum of the resonance. Fig. 6 shows, in solid green, the Q-factor extracted from the measurement results for a resonance near 1550 nm. The quality factor can also be estimated by

$$Q = \frac{\pi n_g L\sqrt{ta}}{\lambda_{res}(1-ta)}. \tag{4}$$

We can express the round trip loss as

$$a = e^{-\alpha/2L}.a', \tag{5}$$

where a' represents the additional field loss caused by the directional coupler in the broken ring. A good fit between the

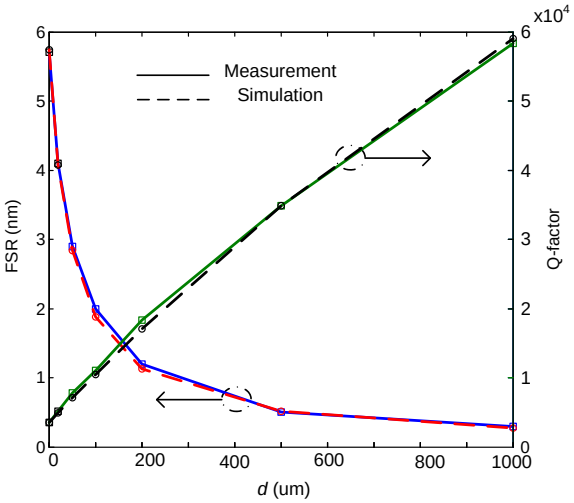

Fig. 6. Measured and simulated FSR and quality factor of the broken racetrack resonator versus displacement, d, based on 7 fabricated samples.

Q-factor obtained from (4) and that from experimental results is achieved by assuming a loss coefficient of $\alpha = 3.5$ dB/cm in silicon waveguides and $a' = 0.94$. The round trip loss and ring transmission coefficient are also consistent with values obtained from the method introduced in [11]. The broken ring has a lower Q-factor compared to conventional microring resonators due to the additional loss suffered in the directional couplers, denoted by a' in (5). Using a larger gap decreases the optical loss and enhances the Q [12].

The ring can be made larger to achieve smaller FSR values. Waveguide propagation loss limits the largest practical ring size. As demonstrated in [4], FSRs smaller than 100 GHz are possible in large silicon-nitride rings. In our experiments, we noticed that the filter extinction ratio decreases in larger rings. This means that the critical coupling condition is no longer valid since larger rings have more loss. To solve this problem, a MEMS actuator can be used to fine tune the coupling coefficient between the bus waveguide and the microring [13]. The coupling coefficient can also be controlled dynamically by using thermal or electro-optic interferometeric couplers to meet the critical coupling condition as shown in [14].

Larger FSRs are possible by reducing the microring dimensions. Ring resonators with radius as small as 1.5 μm have been reported in the [12]. The crossover length can also be reduced by decreasing the gap in directional couplers or by employing waveguides with lower electric field confinement. With careful design we can expect FSRs as large as 20 nm.

The main benefit of the proposed broken racetrack is the possibility of using a MEMS structure to move the inner part of the ring. Among a plethora of MEMS devices, an inchworm motor offers the range of motion (several millimeters) and precision (4 nm) required in this paper [15]. Fig. 7 shows an in-plane inchworm device as proposed by Penskiy et al. [9] with four actuators arranged with symmetry on both sides of a shuttle that carries the movable inner segment of the racetrack. The symmetry of applied forces and addition of a couple of anchor points ensures that the shuttle only travels in

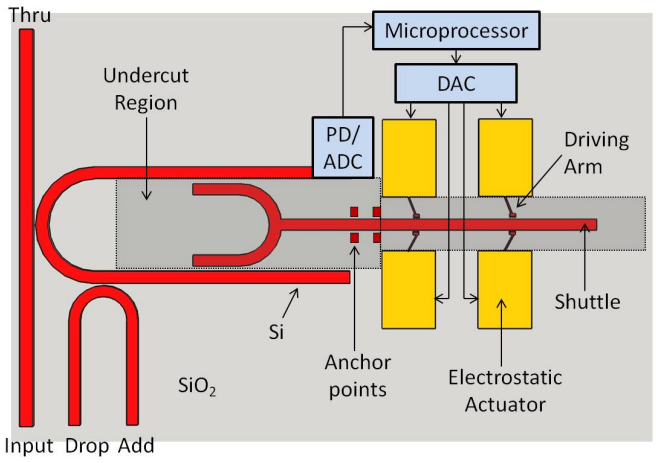

Fig. 7. Block diagram of the MEMS structure and the electronic feedback circuit. PD: photodetector, ADC: analog-to-digital converter. DAC: digital-to-analog converter.

one dimension with very high precision. The shuttle width is narrow enough not to support any optical mode as it connects to the ring segment to avoid light coupling to the shuttle. An optional optical bus can be coupled to the fixed segment of the racetrack for add/drop functionality. An electronic feedback circuit consisting of a photodetector at the monitoring port and a microprocessor can be used to precisely control the actuators and therefore the FSR.

IV. Conclusion

In conclusion, we proposed a novel broken racetrack structure that splits the ring into two physically separate but optically coupled parts. We showed both in simulation and with experimental results that this structure has a good performance as a filter with FSR tunable from 5.7 nm to 0.3 nm. Using a MEMS device to move the arm will result in a compact filter with highly tunable FSR. Such a filter has applications in generating tunable frequency combs, add/drop multiplexers and switches with tunable channel spacing, and tunable RF tone generation.

Acknowledgment

The devices were fabricated at the University of Washington Microfabrication/Nanotechnology User Facility, a member of the NSF National Nanotechnology Infrastructure Network.

References

[1] B. E. Little, S. T. Chu, H. A. Haus, J. Foresi, J. -P. Laine, "Microring resonator channel dropping filters," *J. Lightwave Technol.* 15, 998-1005,1997.

[2] W. Bogaerts, P. De Heyn, T. Van Vaerenbergh, K. De Vos, S. K. Selvaraja, T. Claes, P. Dumon, P. Bienstman, D. Van Thourhout, and R. Baets, "Silicon microring resonators." *Laser and Photonics Reviews* 6, no. 1, 47-73, 2012.

[3] Y. Vlasov, W. M. Green, and F. Xia, "High-throughput silicon nanophotonic wavelength-insensitive switch for on-chip optical networks," *Nature Photonics*, 2(4), 242-246, 2008.

[4] A. Johnson, Y. Okawachi, J. Levy, J. Cardenas, K. Saha, M. Lipson, and A. Gaeta, "Chip-based frequency combs with sub-100 GHz repetition rates," *Opt. Lett.* 37, 875-877, 2012.

[5] J. Magné, P. Giaccari, S. LaRochelle, J. Azaña, and L. R. Chen, "All-fiber comb filter with tunable free spectral range," *Opt. Lett.* 30, 2062-2064, 2005.

[6] A. Atabaki, B. Momeni, A. Eftekhar, E. Hosseini, S. Yegnanarayanan, and A. Adibi, "Tuning of resonance-spacing in a traveling-wave resonator device," *Opt. Express* 18, 9447-9455, 2010.

[7] T. Ikeda, K. Hane, "A microelectromechanically tunable microring resonator composed of freestanding silicon photonic waveguide couplers," *Appl. Phys. Lett.* 102 (2013)221113.

[8] H. M. Chu, K. Hane, "A wide-tuning silicon ring-resonator composed of coupled freestanding waveguides," *IEEE Photon. Technol. Lett.* 26 (2014) 1411-1413.

[9] I. Penskiy, and S. Bergbreiter,"Optimized electrostatic inchworm motors using a flexible driving arm," *J. Micromechanics and Microengineering*, vol. 23, no. 1, p. 015018, Jan. 2013.

[10] N. Rouger, L. Chrostowski, and R. Vafaei, "Temperature Effects on Silicon-on-Insulator (SOI) Racetrack Resonators: A Coupled Analytic and 2-D Finite Difference Approach," *J. Lightwave Technol.* 28, 1380-1391, 2010.

[11] W. McKinnon, D. Xu, C. Storey, E. Post, A. Densmore, A. Delge, P. Waldron, J. Schmid, and S. Janz, "Extracting coupling and loss coefficients from a ring resonator," *Opt. Express* 17, 18971-18982, 2009.

[12] Q. Xu, D. Fattal, and R. Beausoleil, "Silicon microring resonators with 1.5-m radius," *Opt. Express* 16, 4309-4315, 2008.

[13] J. Yao and M. Wu,"Bandwidth-tunable adddrop filters based on micro-electro-mechanical-system actuated silicon microtoroidal resonators," *Opt. Lett.* 34, 2557-2559, 2009.

[14] L. Chen, N. Sherwood-Droz, and M. Lipson,"Compact bandwidth-tunable microring resonators," *Opt. Lett.* 32, 3361-3363, 2007.

[15] P. R. Ouyang, R. C. Tjiptoprodjo, W. J. Zhang, and G. S. Yang, "Micro-motion devices technology: The state of arts review," *The International Journal of Advanced Manufacturing Technology* 38, 463-478, 2008.